J Incl Phenom Macrocycl Chem (2013) 75:247–254
DOI 10.1007/s10847-012-0106-z

ORIGINAL ARTICLE

Vibrational dynamics and hydrogen bond properties of β-CD nanosponges: an FTIR-ATR, Raman and solid-state NMR spectroscopic study

F. Castiglione · V. Crupi · D. Majolino · A. Mele · W. Panzeri · B. Rossi · F. Trotta · V. Venuti

Received: 4 November 2011 / Accepted: 2 January 2012 / Published online: 4 March 2012

Abstract Cyclodextrin nanosponges (CDNS) are cross-linked polymers with remarkable inclusion/release properties. CDNS show swelling capability and a hydrophilicity/hydrophobicity balance that can be dramatically modified by the type and quantity of cross-linking agents. Here, we focus our attention on samples of β-cyclodextrin nanosponges (β-CDNS) obtained by reacting β-cyclodextrin (β-CD) with the cross-linking agent carbonyldiimidazole at different β-CD:cross-linking agent molar ratio. The vibrational properties of CDNS thus synthesized have been investigated by Fourier transform infrared spectroscopy in attenuated total reflectance geometry and Raman spectroscopy in the dry state at room temperature. The quantitative analysis of the O–H stretching region (3,000–3,800 cm^{-1}) allowed us to obtain structural information on the role played by primary and secondary OH groups in the hydrogen bond network of the polymer. Also, the contribution of interstitial and intracavity crystallization water molecules is reported. Solid-state NMR spectroscopy is used to study the molecular mobility of the polymer by measuring the ^1H spin–lattice relaxation time in the rotating frame ($T_{1\rho}$). The $T_{1\rho}$ values obtained for the polymer β-CDNS are compared with free β-CD. The observed relaxation parameters point out that the ester formation occurs mainly at the primary OH groups of CDs, also supporting the interpretation of vibrational spectra.

Keywords Cyclodextrin nanosponges · FTIR-ATR spectroscopy · Raman spectroscopy · O–H stretching · Solid state NMR spectroscopy

F. Castiglione · A. Mele
Dipartimento di Chimica, Materiali e Ing. Chimica "G. Natta", Politecnico di Milano, via Mancinelli 7, 20131 Milano, Italy

V. Crupi · D. Majolino · V. Venuti
Dipartimento di Fisica, Università di Messina, and CNISM, UdR Messina, Viale Ferdinando Stagno D'Alcontres 31, 98166 Messina, Italy

A. Mele
CNR-Istituto di Chimica del Riconoscimento Molecolare, Milano, Italy

W. Panzeri
CNR-Istituto di Chimica del Riconoscimento Molecolare, Sez. Quil., 20131 Milano, Italy

B. Rossi (✉)
Dipartimento di Fisica, Università di Trento, via Sommarive 14, 38123 Povo, Trento, Italy
e-mail: rossi@science.unitn.it

F. Trotta
Dipartimento di Chimica IFM, Università di Torino, via Pietro Giuria, 10125 Torino, Italy

Introduction

Cyclodextrins (CDs) are cyclic oligomers of amylose with hydrophobic cavity that can include and stabilize a large variety of organic molecules by the establishment of non covalent interactions [1]. The capability of forming stable inclusion complexes opened the route to a large number of applications of CDs, with paradigmatic examples, even if not exhaustive, in the field of drug formulation and delivery. However, the use of CDs *tout court* as hosts for the preparation of inclusion complexes suffers from two major drawbacks: the easy dissociation of the complex on dilution, and the polarity and size requirements for the guest molecules that exclude the complexation of hydrophilic or high-molecular-weight molecules.

For these reasons, in recent years many efforts have been addressed at producing more efficient cylcodextrins-based

host systems, following several different strategies, such as dimerization and oligomerization of CDs, and the praparation of synthetic polymers conjugates. Cyclodextrin nanosponges (CDNS) are nanoporous, cross-linked polymers synthesized by reacting cyclodextrins, (β-cyclodextrin, β-CD, only in the present study) with activated carbonyl compounds such as, diisocyanates, carboxylic acids dianhydrides, or synthetic equivalents of phosgene [2–7]. CDNS exhibit interesting inclusion/release properties that have been exploited in a variety of fields, including bio-catalysis, agriculture, environmental control [8–11] and pharmaceutical applications such as nano-vectors or protecting agents for active pharmaceutical ingredients [12–14].

CDNS are insoluble in water and in organic solvents, but some classes of CDNS may swell in the presence of aqueous solutions. A careful choice of the cross-linking agent allows to modulate the swelling properties, ranging from totally unswellable systems to highly swellable polymers able to form gels [7]. In the case of CDNS prepared from pyromellitic anhydride (PMA), we showed that the swelling capability and hydrophilicity/hydrophobicity properties are strongly influenced by the CD:PMA molar ratio. As previously reported, the ease of synthesis of CDNS and the ever growing applications for these novel materials are in striking contrast with the poor knowledge of the structural features of the polymeric network. At the present moment, quantitative data on the distribution of the pore size dimensions are still missing, and the detailed reaction pathway of CDs to afford CDNS is still to be thoroughly investigated. Few experimental studies aimed at working out any long-range order motif within the CDNS frame and inclusion properties of CDNS has been reported so far [5–7]. Again, it is still not clear how the ratio between cross-linking agent and CD during the synthesis of polymers can control the degree of cross-linking (i.e. rigidity) of the final product, and how this property is strictly connected to the swelling ability and inclusion/release properties of the material.

The deep understanding of the structural and dynamical features of CDNS is the first key step for clarifying the mechanism of entrapment of substrates within the polymeric network and their transport properties. In the present paper, we employ three different spectroscopic techniques: Fourier transform infrared spectroscopy in attenuated total reflectance geometry (FTIR-ATR), Raman and nuclear magnetic resonance (NMR) in the solid state to study the molecular mobility and the vibrational properties of the β-CDNS polymers. FTIR-ATR and Raman spectroscopies are used to investigate the vibrational processes of four CDNS obtained from β-CD and carbonyldiimidazole (CDI) (see Fig. 1) at different β-CD:CDI molar ratios. The main purpose is to establish a correlation, if any, between the different vibrational dynamics of the four samples with the

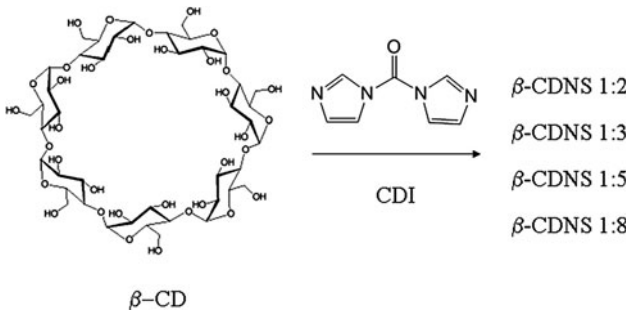

Fig. 1 Scheme of the synthesis of β-CDNS. The numbers refer to the molar ratio between reagents (e.g. β-CDNS 1:2 = polymer obtained from β-CD and CDI in molar ratio 1:2, respectively)

degree of cross-linking of the polymer. A complementary picture is obtained by means of cross-polarization magic angle spinning solid-state nuclear magnetic resonance (CPMAS-NMR) spectroscopy [15–17] and variable contact time (VCT) CPMAS technique. The comparison of the chemical shifts of C atoms in CDNS and in native CD, and the determination of relaxation parameters such as ^{1}H $T_{1\rho}$ (the ^{1}H spin–lattice relaxation in the rotating frame) provide valuable insights for the understanding of the chemical structure and dynamics of the nanosponges. NMR data also support the interpretation of the observed changes in the vibrational spectra of CDNS as varying the cross-linking degree of the polymers.

Experimental

Materials

In order to obtain β-CDNS 1:n nanosponges (see Fig. 1 for the adopted nomenclature), the reactions of polymerization between β-CD and cross-linking agent CDI at molecular ratios of 1:n (with $n = 2, 3, 5, 8$) were conducted dissolving β-CD in anhydrous CDI. Once added the required molar amount of CDI, the mixture was allowed to react for 4 h at $T = 100$ °C. Once the reaction was over, a great excess of water was added and the solid recovered by filtration under vacuum, washed with ethanol and then Sohxlet extracted with ethanol for 10 h.

Methods

FTIR-ATR spectroscopy

FTIR-ATR spectra were collected, at room temperature, in the 400–4,000 cm^{-1} region. Measurements were performed using a Bomem DA8 Fourier transform spectrometer, operating with a Globar source, in combination with a KBr beamsplitter and a thermoelectrically cooled

deuterated triglycene sulphate (DTGS) detector. A Golden Gate diamond ATR system, just based on the attenuated total reflectance (ATR) technique, contained the powders [18]. An ATR set-up exhibits various advantages with respect to an ordinary absorption setup. It is non-destructive, it requires only micrograms of sample, and it is at the origin of spectra displaying a very good signal to noise ratio, being in particular easy to avoid saturation of bands. In addition, a chemical analysis can be performed directly on ATR spectra, avoiding implementation of elaborated calculations of optical constants. Spectra were recorded in dry atmosphere, by co-addition of 100 repetitive interferograms at a resolution of 4 cm^{-1} and then normalized for taking into account the effective number of absorbers. To check a possible unwanted effect induced by wetting and/or drying phenomena when the sample holder was filled with dry nitrogen, IR spectra in the presence and absence of air were compared without showing any significant difference. No mathematical correction (e.g. smoothing) was done, and spectroscopic manipulation such as baseline adjustment and normalization were performed using the Spectracalc software package GRAMS (Galactic Industries, Salem, NH, USA).

The analysis of the 3,000–3,800 cm^{-1} region, typical of the O–H stretching intramolecular vibrational mode, which required a band decomposition procedure, was undertaken using second derivative computations for evaluating the wavenumbers of the maxima of the different sub-bands. Multiple curve fitting was then applied to the experimental profiles based on these wavenumber values, by using the routine provided in the PeakFit 4.0 software package. It enabled the type of fitting function to be selected and allowed specific parameters to be fixed or varied accordingly. The strategy adopted was to use well-defined shape components of Voigt functions with all the parameters allowed to vary upon iteration until converging "best-fit" solution is reached. The procedure adopted makes use of the minimum number of parameters. The "best-fit" is characterized by $r^2 \approx 0.9999$ for all the investigated systems.

Raman spectroscopy

Raman spectra of β-CDNS were recorded on dried samples deposited on a glass slide, in air, at room temperature, by means of a microprobe setup (Horiba-Jobin–Yvon, LabRam Aramis) consisting of a He–Ne laser, a narrow-band notch filter, a 46 cm focal length spectrograph using a 1800 grooves/mm grating and a charge-coupled device (CCD) detector. Exciting radiation at 632.8 nm was focused onto the sample surface with a spot size of about 1 μm^2 through a 100× objective with NA = 0.9. To avoid unwanted laser-induced transformations, neutral filters of different optical densities were used, whenever necessary. Spectra were collected in the wavenumber ranges 100–3,700 cm^{-1}. The resolution was about 0.35 cm^{-1}/pixel.

NMR spectroscopy

Solid-state CP/MAS ^{13}C NMR spectra were recorded at 298 K on a Bruker Avance 600 spectrometer, operating at a frequency of 150.9 MHz and equipped with a MAS probe head. The powder sample was inserted in a 4 mm zirconia rotor and spun in air at 8 kHz. The CP Hartmann-Hahn condition was established using the standard glycine sample and adamantine was used as chemical shift reference. The conventional ^{13}C spectra were recorded with a proton 90° pulse length of 4 μs, a contact time of 1 ms and 4 s as recycle delay time. Each free induction decay (FID) was acquired with 512 scans and a sweep width of 250 ppm. ^{1}H TPPM [19] decoupling was used during the acquisition period. VCT experiments were performed with the contact times, t_m in the range 0.06–5 ms.

Results and discussion

Vibrational spectroscopy

The combined use of Raman and Infrared spectroscopy can provide complementary information on the vibrational dynamics of a molecular system; in fact, although some vibrations may be active in both Raman and IR spectra, the corresponding vibrational bands can appear more or less intense depending on the spectroscopic technique that is used.

The broad band due to the O–H stretching is a good probe of hydrogen bonding structural network, because a change of the relative populations of differently H-bonded molecules is revealed by a change in its shape and position [20–22]. The quantitative spectroscopic investigation of this band is achieved by a fitting procedure accounting for the different components corresponding to different species: primary and secondary OH groups of CD, interstitial and intracavity water molecules. Band deconvolution provides the relative populations of the different spectral species by the analysis of the intensity of the corresponding sub-bands, and the strength of the H-bond of the hydroxyl groups determining their frequency position.

In Fig. 2a–b we report the Raman and FTIR-ATR spectra collected in the O–H stretching region for all the analysed samples, respectively. As general qualitative trend, by increasing the cross linking agent the O–H band tends to move to higher frequency, as observed both in Raman and IR spectra. This indicates a change in the hydrogen bond scheme, that implies a reduced co-operativity involving shorter lifetimes, in agreement with other previous studies [21–23].

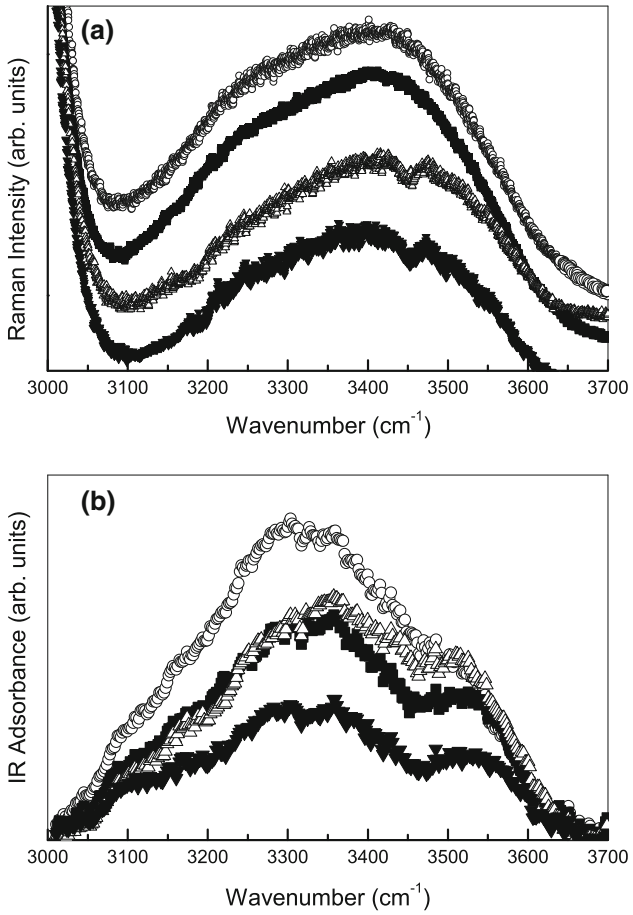

Fig. 2 Raman (**a**) and FTIR-ATR (**b**) spectra in the O–H stretching region of β-CDNS in 1:2 (*open circles*), 1:3 (*closed squares*), 1:5 (*open up triangles*), 1:8 (*closed down triangles*) β-CD:CDI molar ratio

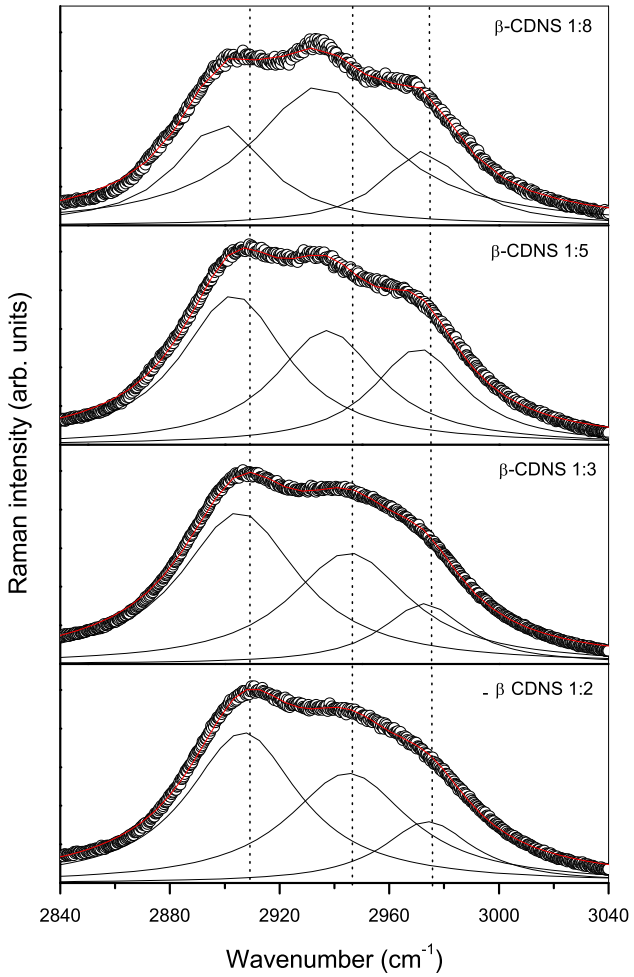

Fig. 3 Raman spectra in the C–H stretching region of β-CDNS obtained with different β-CD:CDI molar ratios; experimental data (*empty circles*) and Lorentz fit of the data (*continuous lines*)

A clear evolution in the C–H stretching band, as a function of the β-CD:CDI molar ratio, can be also observed by comparing the Raman spectra of all the examined β-CDNS samples, collected in the wavenumber range between 2,840 and 3,040 cm^{-1} (Fig. 3). For a finer investigation, the spectral contributions in this region were modelled with three modes fitted by using Lorentz functions; in this way, the influence of the cross-linking degree on the spectral changes observed in the CDNS spectra could be readily inspected.

As it is evident in Fig. 3, the amount of cross-linker does not seem significantly affect the intensity and frequency position of the band falling at about 2,975 cm^{-1}; at the contrary, the modes observed at 2,947 and 2,909 cm^{-1} in the spectra of βCDNS 1:2 shift to lower wavenumbers as a consequence of the increasing of the β-CD:CDI molar ratio. These spectral features can be used as a proper marker revealing the different structure of the polymeric network obtained by varying the amount of cross-linker respect to CD. Indeed, the components at 2,947 and 2,909 cm^{-1} (referenced to βCDNS 1:2) are sensitive to the synthetic protocol of the polymer and can be taken as descriptors of the polymerization process, irrespective of the detailed assignment of the components of such C–H stretching bands that is, at moment, not yet available.

The high-quality data obtained by FTIR-ATR technique allowed a quantitative analysis of the observed spectroscopic changes, that required a decomposition of the O–H stretching band in five contributions, interpreted on the basis of previous studies [23–27]. This spectral region is a superposition of the O–H stretching vibrations corresponding to interstitial ($\omega_1 \sim 3{,}146\ cm^{-1}$, $\omega_3 \sim 3{,}322\ cm^{-1}$) and intracavity ($\omega_5 \sim 3{,}528\ cm^{-1}$) water molecules, primary ($\omega_4 \sim 3{,}398\ cm^{-1}$) and secondary ($\omega_2 \sim 3{,}252\ cm^{-1}$) OH groups of the cyclodextrin.

Figure 4 shows the O–H band fitting results for all the investigated samples. The main best-fit parameters of each component, i.e. peak wavenumbers and relative intensities,

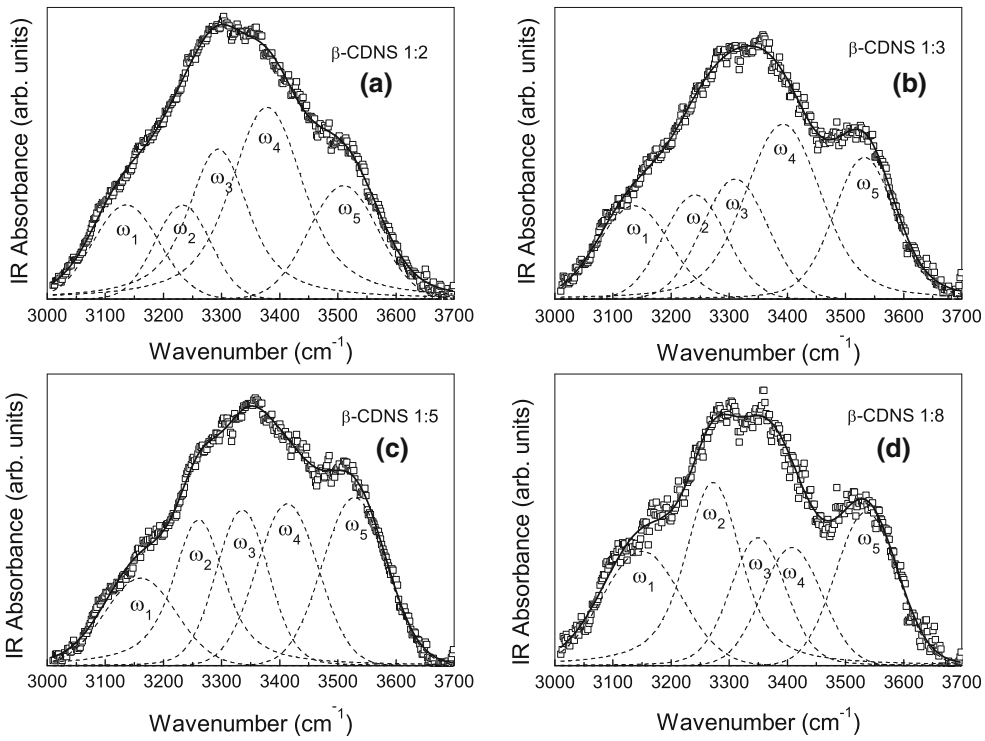

Fig. 4 FTIR-ATR spectrum (*open squares*) in the O–H stretching region of β-CDNS in 1:2 (**a**), 1:3 (**b**), 1:5 (**c**), 1:8 (**d**) β-CD:CDI molar ratio, together with the best-fit (*continuous line*) and the deconvolution components (*dashed lines*)

together with their vibrational assignment, are reported in Table 1.

The peak wavenumbers are related to the connectivity of the corresponding H-bonds: an increase in the number of molecules involved in the network, generally induces a decrease in the frequency of the intramolecular stretching vibration of the OH groups, while the shift of these vibrations to higher wavenumbers indicates the weakening of the hydrogen bonding network, due to the establishment of less intense associations [20, 21].

As a general trend, by increasing the β-CD:CDI molar ratio, a high-frequency shift of all the contributions is observed, indicating a reduction of the co-operativity of the bonds. This could reveal a destructuring effect of the cross-linking agent on the hydrogen bond network of the cyclodextrin units.

The percentage area of the resolved components accounts for the fractional populations of the individual species present. Data of Fig. 5 clearly indicate that the population of the primary OH groups of cyclodextrins decreases with increasing β-CD:CDI molar ratio (decrease of I_4) whereas the opposite trend is observed for the population of secondary OH groups (increase of I_2). The populations of intracavity (I_5) and interstitial water molecules ($I_1 + I_3$) do not seem to be affected by β-CD:CDI molar ratio. At this stage some explanations of these observed trends can be proposed. The primary OH groups of the native CDs are expected to be the most involved in

Table 1 Vibrational assignment and main fitting parameters, i.e. wavenumber (ω, cm^{-1}) and percentage intensity (I, %), of the FTIR-ATR sub-bands in the O–H stretching region of β-CDNS at all the investigated β-CD:CDI molar ratio

O–H stretching intersitital H_2O		O–H stretching secondary OH groups		O–H stretching interstitial H_2O		O–H stretching primary OH groups		O–H stretching intracavity H_2O	
ω_1 (cm^{-1})	I_1 (%)	ω_2 (cm^{-1})	I_2 (%)	ω_3 (cm^{-1})	I_3 (%)	ω_4 (cm^{-1})	I_4 (%)	ω_5 (cm^{-1})	I_5 (%)
β-CDNS 1:2									
3136.0	12.7	3233.1	10.7	3294.2	24.6	3378.3	35.9	3510.0	16.1
β-CDNS 1:3									
3136.3	14.5	3240.9	14.4	3310.0	17.1	3392.6	33.1	3532.6	20.9
β-CDNS 1:5									
3160.7	13.8	3261.0	21.7	3335.5	18.9	3413.3	22.0	3528.6	23.6
β-CDNS 1:8									
3150.0	19.5	3272.2	28.2	3349.6	16.4	3407.9	15.4	3535.7	20.5

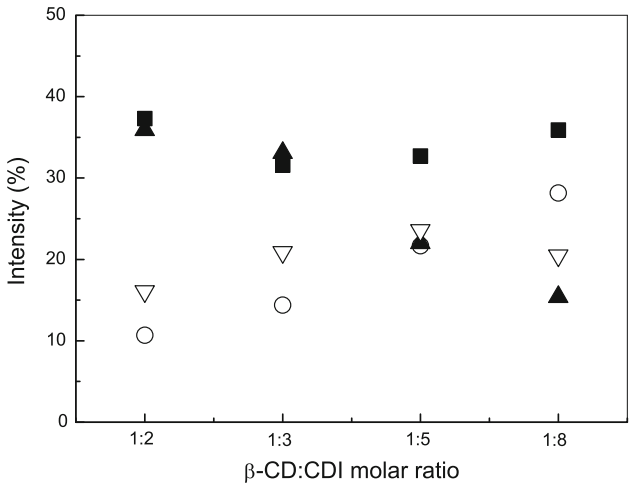

Fig. 5 Relative intensities of the deconvolution components of the experimental FTIR-ATR O–H stretching band for β-CDNS, plotted as a function of β-CD:CDI molar ratio: interstitial H_2O molecules ($I_1 + I_3$, *closed squares*), secondary OH groups (I_2, *open circles*), primary OH groups (I_4, *closed up triangles*), intracavity H_2O molecules (I_5, *open down triangles*)

the polymerization process, thus the decrease of their population suggests an increase of the cross-linking of the polymer for high β-CD:CDI molar ratios. As long as the cross-linking occurs, the total number of free primary OH groups decreases and thus their contribution as free oscillators to the intensity of the OH stretching band decreases. For the time being, this is the first direct proof of the regioselectivity of the chemical derivatization of CD during the nanosponge synthesis and thus represent an important achievement for the basic knowledge of the molecular structure of these systems.

The increase of the population of secondary OH groups with increasing β-CD:CDI molar ratios is more puzzling. It could be interpreted as a destructuring effect on the intramolecular H-bond network of the individual CD units, most likely due to steric effects. The more sterically congested the nanosponge is, the more distorted the macrorings are expected to be. The disruption of the internal H-bond networks makes the overall number of free secondary OH groups increasingly larger, with consequent increase of their contribution to the stretching band.

Finally, a comment on the component related to the water molecules is due. As a matter of fact the population of interstitial and intracavity water molecules seems to be independent of the polymerization course. Although we cannot provide a clear-cut explanation at this stage, it seems reasonable assuming that the modifications of the molecular environment due to the three-dimensional growth of the CDNS do not affect the local environment experienced by the water molecules and thus the vibrational behaviour. This point will be further investigated in the follow-up of this research.

^{13}C CP/MAS NMR spectroscopy

Molecular assignment of the ^{13}C CP/MAS spectrum of β-CDNS 1:3 is based on the values reported in literature for the crystalline β-CD [28]. Four carbon resonances are observed, which in the order of decreasing resonance frequency, are C(1), C(4), [C(5), C(3), C(2) overlapping lines] and C(6), respectively. All the resonances appear mainly as broad single peaks, while the C(6) carbon gives two broad peaks (C6a) and (C6b) respectively. We measured the ^{13}C chemical shift differences between the native β-CD and the corresponding CDNS polymer to probe the structural modifications induced on the β-CD by the nanosponge polymer formation. The signals of C(1), C(4), [C(5), C(3) and C(2)] do not show any chemical shift change suggesting that the local environments of the sugar ring is very similar to that of native β-CD after polymer formation. For the C(6) carbon, a valuable chemical shift variation respect to the CD precursor is observed (see Table 2). This result clearly indicates a certain degree of structure deformation and the possibility that there are two species coexisting in powder CDNS compounds.

The VCT ^{1}H-^{13}C CP/MAS spectra of β-CDNS 1:3 were acquired and the dependence of the individual ^{13}C peak intensities on the contact times is plotted in Fig. 6. The CP kinetics is reported as the dependence of the peak intensity I(t) on the contact time t [29]. Since the CP process is based on heteronuclear dipolar interactions, it is sensitive to internuclear distances and the mobility of molecules, then can be used to monitor the molecular dynamics in solids. Basically, two spin relaxation processes govern the CP transfer: T_{CH}, the cross-relaxation time and $T_{1\rho}$, the spin lattice relaxation of the protons in the rotating frame. The former dominates the rising, initial part of the curve of signal intensity versus contact time, whilst the latter governs the decaying part of the same curve. Both parameters are sensitive to the local motion and are related to the signal intensity I(t) by Eq. 1:

$$I(t) = I_0\left(1 - \frac{T_{CH}}{T_{1\rho H}}\right)^{-1}\left[\exp\left(-t/T_{1\rho H}\right) - \exp\left(-t/T_{CH}\right)\right] \quad (1)$$

Equation 1 was fitted to the experimental data to obtain the $T_{1\rho}$ for each resolved carbon atom. The results are

Table 2 ^{13}C chemical shift (ppm) for β-CD and β-CDNS 1:3

β-CD	^{13}C Chemical shift	β-CDNS 1:3	^{13}C Chemical shift
C(1)	103.2	C(1)	102.8
C(4)	81.8	C(4)	81.9
[C(2), C(3), C(5)]	73.8	[C(2), C(3), C(5)]	73.2
C(6)	62.8	C(6a)	61.8
		C(6b)	60.2

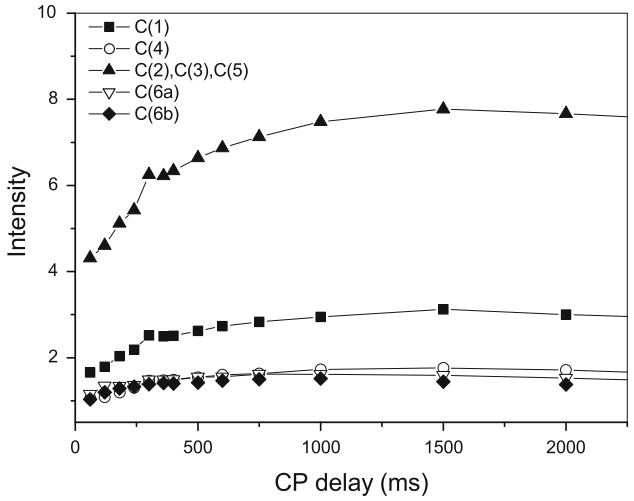

Fig. 6 Cross-polarization (CP) build up curve of the ^{13}C resonances for β-CDNS 1:3 with variable contact time

reported in Table 3 together with the $T_{1\rho}$ values [28] of native crystalline β-CD for comparison. In the latter case, the virtually identical $T_{1\rho}$ values reported for the C atoms of the glucose frame of crystalline native β-CD mean that all the C atoms undergo the same dynamic environment. Conversely, in the present work all the carbon atoms of the sugar ring of β-CDNS showed equivalent $T_{1\rho}$ values but C(6). The latter showed a significantly higher value of $T_{1\rho}$, indicating that molecular mobility around the $-CH_2OH$ groups of CD is affected by polymerization. In other words, the conformational flexybility of the $-CH_2OH$ groups is strongly reduced due to the formation of the ester linkage with the cross-linking agent and formation of the three-dimensional polymer network. In this way, the dynamics of the C(6) atoms of the glucose rings of CD units are made different from those of the C atoms bearing the secondary OH groups, which are not directly involved in the cross-linking reaction. This finding is fully consistent with the observed decrease of population of free secondary OH groups with increasing concentration of cross-liker reported in the previous sections and confirms that the reactive sites of CD are mainly the primary OH groups. Further NMR investigation is being done on β-CDNS with different β-CD:DPC molar ratios in order to shed a light on the influence of the cross-linking degree on the NMR parameters discussed above.

Table 3 ^1H spin–lattice relaxation in the rotating frame ($T_{1\rho}$ in ms) of the carbon atoms of native and crystalline β-CD [literature data from ref. 28] and β-CDNS 1:3 [this work]

β-CD	$T_{1\rho}$ (ms)	β-CDNS 1:3	$T_{1\rho}$ (ms)
C(1)	2.6	C(1)	1.8
C(4)	2.4	C(4)	1.4
[C(2), C(3), C(5)]	2.4	[C(2), C(3), C(5)]	1.6
C(6)	2.7	C(6)	2.2

Conclusions

The combined use of resolution vibrational spectroscopies and solid state NMR provided information on the molecular structure and dynamics of CDNS at increasing degree of β-CD:CDI molar ratios. The quantitative analysis of the IR and Raman spectra in the high-frequency region (2,800–3,800 cm^{-1}), where the bands assigned to the stretching vibrations of CH and OH groups fall, revealed successful in clarifying the role played by the cross-linking agent on the H-bonded imposed structural scheme of nanosponges. In particular, the neat trends observed for the primary and secondary OH groups populations with cross-linking degree of the polymer opened the way to a methodological use of such approach to monitor the reaction course of the CDNS preparation. The vibrational data were cross-validated by solid state ^{13}C CP/MAS NMR spectroscopy. Chemical shift and $T_{1\rho}$ changes with respect to standard monomeric and crystalline β-CD were observed for C(6) only, confirming the FTIR data on population of primary OH oscillators and also providing the clear indication of the reactive sites of CD in the CDNS formation.

References

1. Bender, M.L., Komiyama, M.: Cyclodextrin chemistry. Springer, New York (1978)
2. Trotta, F., Tumiatti, W.: Patent WO 03/085002 (2003)
3. Li, D., Ma, M.: New organic nanoporous polymers and their inclusion complexes. Chem. Mater. **11**, 872–874 (1999)
4. Trotta, F., Tumiatti, W., Cavalli, R., Zerbinati, O., Roggero, C. M., Vallero, R.: Ultrasound-assisted synthesis of cyclodextrin-based nanosponges. Patent number WO 06/002814 (2006)
5. Cavalli, R., Trotta, F., Tumiatti, W.: Cyclodextrin-based nanosponges for drug delivery. J. Incl. Phenom. Macrocycl. Chem. **56**, 209–213 (2006)
6. Trotta, F., Cavalli, R.: Characterization and applications of new hyper-cross-linked cyclodextrins. Compos. Interface **16**, 39–48 (2009)
7. Mele, A., Castiglione, F., Malpezzi, L., Ganazzoli, F., Raffaini, G., Trotta, F., Rossi, B., Fontana, A., Giunchi, G.: HR MAS NMR, powder XRD and Raman spectroscopy study of inclusion phenomena in βCD nanosponges. J. Incl. Phenom. Macrocycl. Chem. **69**, 403–409 (2011)
8. Arkas, M., Allabashi, R., Tsiourvas, D., Mattausch, E.-M., Perfler, R.: Organic/inorganic hybrid filters based on dendritic and cyclodextrin ''nanosponges'' for the removal of organic pollutants from water. Environ. Sci. Technol. **40**, 2771–2777 (2006)
9. Mhlanga, S.D., Mamba, B.B., Krause, R.W., Malefetse, T.J.: Removal of organic contaminants from water using nanosponge cyclodextrin polyurethanes. J. Chem. Technol. Biotechnol. **82**, 382–388 (2007)

10. Mamba, B.B., Krause, R.W., Malefetse, T.J., Nxumalo, E.N.: Monofunctionalized cyclodextrin polymers for the removal of organic pollutants fromwater. Environ. Chem. Lett. **5**, 79–84 (2007)
11. Mamba, B.B., Krause, R.W., Malefetse, T.J., Gericke, G., Sithole, S.P.: Cyclodextrin nanosponges in the removal of organic matter to produce water for power generation. Water SA **34**, 657–660 (2008)
12. Swaminathan, S., Vavia, P.R., Trotta, F., Torne, S.: Formulation of beta-cyclodextrin based nanosponges of itraconazole. J. Incl. Phenom. Macrocycl. Chem. **57**, 89–94 (2007)
13. Vyas, A., Shailendra, S., Swarnlata, S.: Cyclodextrin based novel drug delivery systems. J. Incl. Phenom. Macrocycl. Chem. **62**, 23–42 (2008)
14. Ansari, K.A., Vavia, P.R., Trotta, F., Cavalli, R.: Cyclodextrin-based nanosponges for delivery of resveratrol: in vitro characterisation, stability, cytotoxicity and permeation study. AAPS Pharm. Sci. Tech. **12**, 279–286 (2011)
15. Pines, A., Gibby, M., Waugh, J.S.: Proton-enhanced NMR in dilute spins in solids. J. Chem. Phys. **59**, 569–573 (1973)
16. Mehring, M.: High-Resolution NMR Spectroscopy in Solids. Springer, New York (1983)
17. Stejskal, E.O., Memory, J.D.: High-Resolution NMR in the Solid State. Fundamental of CP/MAS. Oxford University Press, Oxford (1994)
18. Maréchal, Y.: Observing the water molecule in macromolecules and aqueous media using infrared spectrometry. J. Mol. Struct. **648**, 27–47 (2003)
19. Bennett, A.E., Rienstra, C.M., Auger, M., Lakshmi, K.V., Griffin, R.G.: Heteronuclear decoupling in rotating solids. J. Chem. Phys. **103**, 6951–6958 (1995)
20. Crupi, V., Longo, F., Majolino, D., Venuti, V.: Vibrational properties of water molecules adsorbed in different zeolitic frameworks. J. Phys. Condens. Matter **18**, 3563–3580 (2006)
21. Crupi, V., Longo, F., Majolino, D., Venuti, V.: T dependence of vibrational dynamics of water in ion-exchanged zeolites A: a detailed Fourier transform infrared attenuated total reflection study. J. Chem. Phys. **123**, 154702 (2005)
22. Mallamace, F., Broccio, M., Corsaro, C., Faraone, A., Majolino, D., Venuti, V., Liu, L., Mou, C.Y., Chen, S.H.: Evidence of the existence of the low-density liquid phase in supercooled, confined water. Proc. Natl. Acad. Sci. USA **104**, 424–428 (2007)
23. Crupi, V., Ficarra, R., Guardo, M., Majolino, D., Stancanelli, R., Venuti, V.: UV–vis and FTIR–ATR spectroscopic techniques to study the inclusion complexes of genistein with β-cyclodextrins. J. Pharm. Biomed. Anal. **44**, 110–117 (2007)
24. Gavira, J.M., Hernanz, A., Bratu, I.: Dehydration of β-cyclodextrin: an IR ν(OH) band profile analysis. Vib. Spectrosc. **32**, 137–146 (2003)
25. Bratu, I., Veiga, F., Fernandes, C., Hernanz, A., Gavira, J.M.: Infrared spectroscopic study of triacetyl-β-cyclodextrin and its inclusion complex with nicapiridine. Spectroscopy **18**, 459–467 (2004)
26. Stancanelli, R., Ficarra, R., Cannavà, C., Guardo, M., Calabrò, M.L., Ficarra, P., Ottanà, R., Maccari, R., Crupi, V., Majolino, D., Venuti, V.: UV–vis and FTIR-ATR characterization of 9-fluorenon-2-carboxyester/(2-hydroxypropyl)-β-cyclodextrin inclusion complex. J. Pharm. Biomed. Anal. **47**, 704–709 (2008)
27. Cannavà, C., Crupi, V., Ficarra, P., Guardo, M., Majolino, D., Stancanelli, R., Venuti, V.: Physicochemical characterization of coumestrol/β-cyclodextrins inclusion complexes by UV–vis and FTIR-ATR spectroscopies. Vib. Spectrosc. **48**, 172–178 (2008)
28. Crini, G., Cosentino, C., Bertini, S., Naggi, A., Torri, G., Vecchi, C., Janus, L., Morcellet, M.: Solid state NMR spectroscopy study of molecular motion in cyclomaltoheptanose (β-cyclodextrin) crosslinked with epichlorohydrin. Carbohydr. Res. **308**, 37–45 (1998)
29. Kolodziejski, W., Klinowski, J.: Kinetics of cross-polarization in solid-state NMR: a guide for chemists. Chem. Rev. **102**, 613–628 (2002)